JACS
JOURNAL OF THE AMERICAN CHEMICAL SOCIETY
Article
pubs.acs.org/JACS

Effects of Ions on Hydrogen-Bonding Water Networks in Large Aqueous Nanodrops

Jeremy T. O'Brien[†] and Evan R. Williams*[,†]

[†]Department of Chemistry, University of California, Berkeley, California 94720-1460, United States

ABSTRACT: Ensemble infrared photodissociation (IRPD) spectra in the hydrogen stretch region (~2800−3800 cm^{-1}) are reported for aqueous nanodrops containing ~250 water molecules and either SO_4^{2-}, I^-, Na^+, Ca^{2+}, or La^{3+} at 133 K. Each spectrum has a broad feature in the bonded-OH region (~2800−3500 cm^{-1}) and a sharp feature near 3700 cm^{-1}, corresponding to the free-OH stretch of surface water molecules that accept two hydrogen bonds and donate one hydrogen bond (AAD water molecules). A much weaker band corresponding to AD surface water molecules is observed for all ions except SO_4^{2-}. The frequencies of the AAD free-OH stretch red-shift with increasingly positive charge, consistent with a Stark effect as a result of the ion's electric field at the droplet surface, and from which the corresponding frequency for water molecules at the surface of neutral nanodrops of this size is estimated to be 3699.3−3700.1 cm^{-1}. The intensity of the AAD band increases with increasing positive charge, consistent with a greater population of AAD water molecules for the more positively charged nanodrops. The spectra of $M(H_2O)_{\sim 250}$, M = Na^+ and I^-, are very similar, whereas those for Ca^{2+} and SO_4^{2-} have distinct differences. These results indicate that the monovalent ions do not affect the hydrogen-bonding network of the majority of water molecules whereas this network is significantly affected in nanodrops containing the multivalent ions. The ion-induced effect on water structure propagates all the way to the surface of the nanodrops, which is located more than 1 nm from the ion.

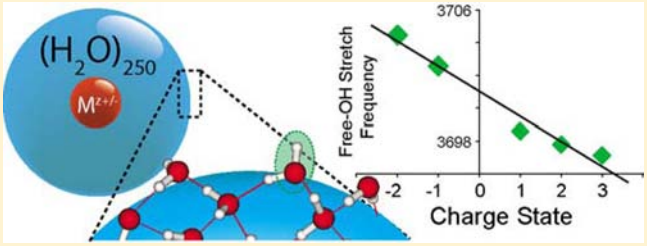

INTRODUCTION

The effects of interactions between ions, proteins, and water have been debated for over 120 years, since Franz Hofmeister first ordered ions by their tendency to precipitate hen egg albumin in aqueous solutions.[1−3] This "Hofmeister series", which ranks how ions affect protein solubility, is remarkably reproducible for a wide variety of salts and proteins and has been observed for other chemical properties, such as salt solubilities,[4] cloud points of nonionic surfactants,[5] and transport through ion channels.[6] Hofmeister series effects have been investigated using a number of methods, including X-ray absorption spectroscopy,[7] nuclear magnetic resonance,[8] sum-frequency generation (SFG) spectroscopy,[9] computational chemistry,[10,11] and static vibrational spectroscopy.[11,12] Results supporting both direct ion−protein interactions[4,7−10,13] and effects of ions on solvent structure[11,14−17] have been reported, but no clear consensus has been reached as to what extent either of these effects are responsible for the Hofmeister series, and the physical origin of this ordering is still debated.[4,7−20]

Recent results from static vibrational spectroscopy,[11,12] femtosecond infrared spectroscopy,[21−24] and terahertz dielectric relaxation spectroscopy[23,24] indicate that ions do not strongly affect the hydrogen bond (H-bond) network of water beyond the first solvation shell for salt solutions with high ionic strengths (2−12 M). Bakker and co-workers reported, on the basis of water reorientation dynamics, that ion−water interactions only extend beyond the first solvation shell in solutions where both ion and counterion are strongly hydrated (i.e., $MgSO_4$).[23,24] They suggest that the physical origin of the Hofmeister series is related to cooperative structure-making effects between ions and charges present on biomolecules.[24]

The effects of salts on water structure at aqueous interfaces have also been linked to the Hofmeister series due to the large dielectric difference at both the liquid−vapor and the protein−water interfaces.[14] Linear spectroscopies have poor sensitivity to surface water molecules due to the overwhelming signal from the bulk. Sum-frequency generation (SFG) spectroscopy is a second-order optical technique, and it is sensitive to the structure of the first few layers of water molecules at the liquid−vapor interface. Results from SFG,[25,26] electrospray ionization,[20] and molecular dynamics simulations[27] indicate that some ions, including Br^- and I^-, are highly surface active,[25,27] whereas other ions, including Cl^-[25] and SO_4^{2-},[26] have lower surface activity, suggesting that the ranking for ion surface activities is similar to that of the Hofmeister series.

Gas-phase studies of hydrated ion clusters have the advantage that the effects of a single ion or electron on water structure can be investigated as a function of hydration extent for up to hundreds of water molecules attached,[28−31] and any competing effects of counterions can be eliminated. The structures of many gas-phase ion complexes, including hydrates of small mono-,[16,31−50] di-,[15,16,47−57] and trivalent[16,28,58] ions have been investigated using infrared photodissociation (IRPD) spectroscopy. Under readily achievable experimental conditions, absorption of a single IR photon by a hydrated ion can induce

Received: April 2, 2012
Published: May 22, 2012

   dx.doi.org/10.1021/ja303191r | J. Am. Chem. Soc. 2012, 134, 10228−10236

a measurable increase in the rate of dissociation, resulting in IRPD spectra that closely resemble linear absorption spectra. Thus, IRPD spectroscopy can be a more direct probe of vibrational resonances than nonlinear spectroscopic methods, such as SFG, and can provide detailed information about both the interior and surface H-bond structure of water in clusters. The hydrogen-stretch region (~2300−4000 cm^{-1}) is especially useful for investigating how ions affect water structure because the frequencies of OH stretching modes are very sensitive to their H-bonding environment. IRPD spectra of small hydrated ion clusters[33−57] indicate that many ions can have strong effects on the structure of water molecules in the first solvation shell, but with some ions, such as tetramethylammonium[32] and Cs^+,[37] water−water hydrogen bonding is favored over ion−water interactions, and these ions have little effect on the hydration structure. Results from IRPD spectroscopy of hydrated SO_4^{2-} indicate that the dianion strongly affects water structure even beyond the second solvation shell for clusters with up to 80 water molecules attached, which contrasts sharply with conclusions from condensed phase femtosecond spectroscopy studies.[15] Recent results from IRPD spectroscopy of 17 different hydrated ions with charge states between −1 and +3 at fixed cluster size (35−37 water molecules) show spectral differences attributable to various extents of ion-induced patterning of the water network that extends to the surface of the clusters, providing further evidence of long-range ion effects on hydration structure.[16]

Here, we present results from IRPD spectroscopy of $M(H_2O)_{\sim 250}$, where M = La^{3+}, Ca^{2+}, Na^+, I^-, and SO_4^{2-} in the spectral region 2800−3800 cm^{-1} measured at 133 K. To our knowledge, these are the largest mass-selected ionic clusters for which IRPD spectra have been reported. These spectra indicate that ion-induced patterning of the water network extends to the surface of these nanodrops and that the surface free-OH stretch frequency depends on ion charge state. Effects of ion polarity and charge state are investigated and compared to results for smaller hydrated ions as well as to condensed-phase results.

EXPERIMENTAL SECTION

All experiments were performed on a home-built 7.0 T Fourier-transform ion cyclotron resonance (FT/ICR) mass spectrometer coupled with a tunable OPO/OPA laser system. The instrument and experimental setup, which previously included a 2.75 T magnet, are described in detail elsewhere.[59] Briefly, hydrated ion clusters are generated by nanoelectrospray ionization of 2−6 mM aqueous solutions using borosilicate capillaries pulled to an inner tip diameter of ~1 μm that are filled with the solution of interest. A platinum wire is inserted into the capillary so that it is in contact with the solution, and a voltage of ~+600 V relative to the entrance of the mass spectrometer is applied to the wire. Hydrated ions are guided through five stages of differential pumping to an ion cell surrounded by a temperature controlled copper jacket, cooled using a regulated flow of liquid nitrogen to 133 K. The temperature of the copper jacket is equilibrated for at least 8 h prior to each experiment. Ions are accumulated for 3−6 s and thermalized with the aid of a pulse of dry nitrogen gas (~10^{-6} Torr). After a 6−12 s delay, the pressure in the ion cell returns to <10^{-8} Torr and the ions of interest are isolated using a stored inverse Fourier transform waveform.

IRPD spectra are obtained using the ensemble average method, which improves the signal-to-noise ratio of IRPD spectra compared to spectra measured for an individual ion.[60] Ensembles of hydrated ions containing 245−255 water molecules are isolated and irradiated with tunable light from an OPO/OPA laser system (LaserVision, Bellevue, WA, U.S.A.) pumped by a 1064 cm^{-1} Nd:YAG laser (Continuum Surelite I-10, Santa Clara, CA, U.S.A.) at a 10 Hz repetition rate for 0.5−1 s. Background dissociation due to blackbody infrared radiative dissociation (BIRD) and changes in the initial ensemble distribution are remeasured approximately every 10 min. BIRD rate constants (k_{BIRD}) are measured in the absence of laser irradiation and calculated from the measured ion abundances.

$$k_{BIRD} = ((\langle n(t)\rangle - \langle n(0)\rangle)/t)$$

$\langle n(t)\rangle$ is the abundance-weighted average number of water molecules in the ensemble after exposure to the 133 K blackbody field for time t. Laser-induced photodissociation rate constants (k_{IRPD}) are calculated similarly, where t_{irr} is the laser irradiation time and $\hbar\omega$ is the laser photon energy.

$$k_{IRPD}(\hbar\omega, t_{irr}) = ((\langle n(\hbar\omega, t_{irr})\rangle - \langle n(0)\rangle)/t_{irr}) - k_{BIRD}$$

k_{IRPD} is plotted versus photon energy to obtain the average IRPD spectrum of the isolated ensemble of hydrated ions. All ensemble IRPD spectra are corrected for frequency-dependent variations in laser power by scaling each k_{IRPD} value by the laser power at that energy.

Calculated structures of $Ca^{2+}(H_2O)_{250}$ and $SO_4^{2-}(H_2O)_{250}$ are obtained to compare the average number of free-OH groups present in each cluster. After an initial geometry relaxation using molecular mechanics, canonical ensemble molecular dynamics is used to generate 1000 structures for each hydrated ion cluster at 133 K using Impact 5.6 (Schrödinger, LLC, Portland, OR). Every atom is assigned an electrostatic charge, +0.41/−0.82e, for hydrogen and oxygen, respectively, and the ion is assigned its full formal charge. The projection E_i of the local electric field at a given hydrogen atom (H_i) onto a unit vector in the OH_i direction is calculated on the basis of contributions from the ion and the hydrogen and oxygen atoms of all other water molecules. The distribution of E_i values obtained is bimodal, corresponding to contributions from free-OH and bonded-OH groups. The average number of free-OH groups is obtained from the histogram of E_i values for all 1000 structures. A similar technique has been applied previously to calculate infrared absorption spectra of hydrated ion clusters containing 36 water molecules.[16]

RESULTS AND DISCUSSION

Hydrated Ion Formation. Under "soft" instrumental conditions, a broad distribution of hydrated ions can be formed using electrospray ionization from aqueous solutions and trapped in the cooled ion cell of a FT/ICR mass spectrometer. A typical mass spectrum measured under such conditions of $La^{3+}(H_2O)_n$ with as many as 500 water molecules attached is shown in Figure 1, illustrating the much larger clusters that can be detected with a 7.0 T magnet compared to previous results with a 2.7 T magnet on this same instrument. Because of the wide range of clusters produced and the limited ion storage capabilities of the cell, the abundance of any individual cluster is relatively low. In addition, the blackbody infrared radiative dissociation (BIRD) rate for large clusters is high, which makes it challenging to isolate and measure the IRPD spectrum of a single cluster size with a high signal-to-noise (S/N) ratio. IRPD spectra were measured using the ensemble average method[60] with an initial distribution of clusters with ~245−255 water molecules. In addition to increasing S/N ratios, this method has the advantage that the potential influence of a single "magic" number cluster on the IRPD spectra is significantly reduced, although such effects are likely to be negligible for clusters of this size.

Spectroscopy. IRPD spectra of $M(H_2O)_{\sim 250}$ at 133 K, where M = La^{3+}, Ca^{2+}, Na^+, I^-, and SO_4^{2-} in the spectral region 2800−3800 cm^{-1}, are shown in Figures 2 and 3. The spectrum for each ion has a broad feature that extends from 2950 to 3675 cm^{-1}, which is attributable to H-bonded OH groups. There is also a narrow band near 3700 cm^{-1}, which is due to free-OH

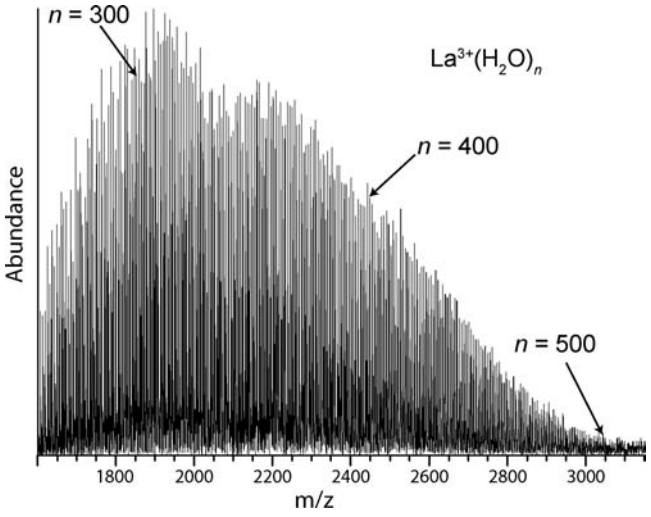

Figure 1. Representative electrospray ionization mass spectrum of a 4 mM aqueous $LaCl_3$ solution with the copper jacket surrounding the ion cell at 133 K. $La^{3+}(H_2O)_n$ nanodrops with ~250−500 water molecules are observed.

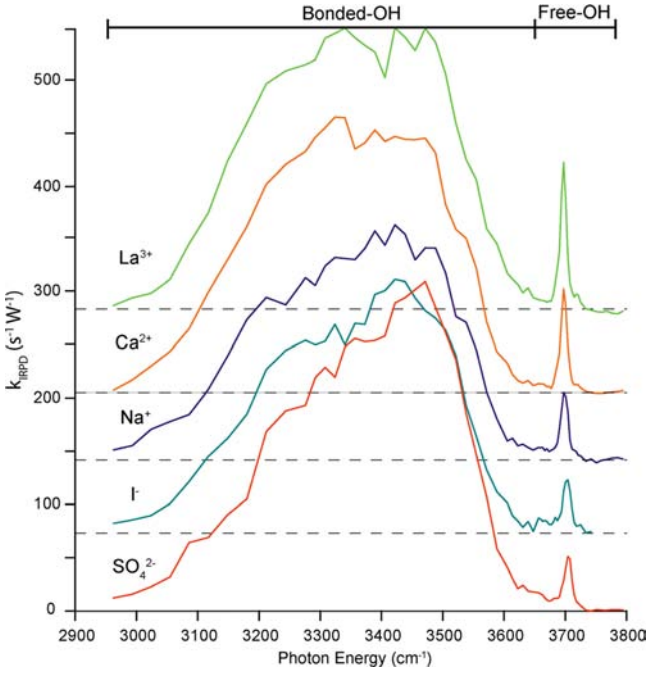

Figure 2. Ensemble IRPD spectra of $M(H_2O)_{\sim 250}$: M = La^{3+}, Ca^{2+}, Na^+, I^-, and SO_4^{2-} at 133 K.

stretches of water molecules that accept two H-bonds and donate one H-bond (defined as an AAD water molecule). A small shoulder band is present at slightly higher frequencies, near 3720 cm^{-1}, for each ion except SO_4^{2-}, and is due to water molecules that accept and donate a single H-bond (AD water molecules). The centroids of the H-bonded features and the free-OH bands vary between 3300 and 3400 cm^{-1} and between 3697 and 3705 cm^{-1}, respectively. The spectra of these clusters are similar owing to the large number of water molecules and the similar local H-bonding environments for many of the water molecules. However, even at this large cluster size (roughly equivalent to a bulk single ion concentration of 200 mM), there are distinct spectral differences that indicate the various extents to which ions can affect the H-bonding network

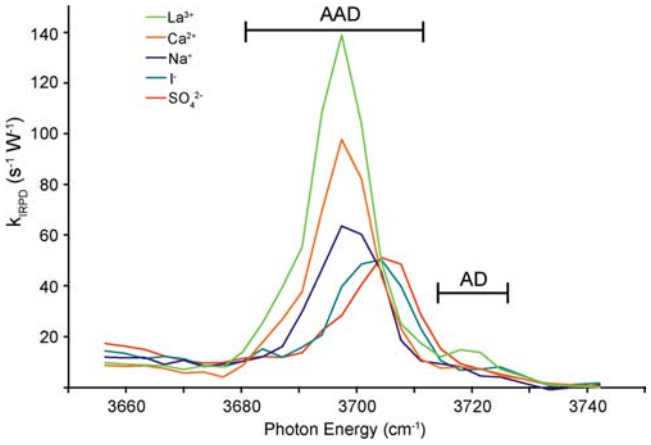

Figure 3. Ensemble IRPD spectra in the free-OH region for $M(H_2O)_{\sim 250}$: M = La^{3+}, Ca^{2+}, Na^+, I^-, and SO_4^{2-} at 133 K.

of water molecules, even for those molecules that are remote from the ion.

The IRPD spectra of the $M(H_2O)_{\sim 250}$ nanodrops more closely resemble the IR absorbance spectra of liquid water or amorphous ice than that of crystalline ice.[61] In the absence of an ion, the nanodrop's freezing point is estimated from the Gibbs−Thomson equation and an approximate diameter of 2.4 nm to be ~234 K. Results from IR spectroscopy of water droplets in a supersonic expansion indicate that the onset of freezing occurs at ~202 K for a 3.2 nm droplet.[62] The presence of an ion in the nanodrop should further reduce the freezing point. Binding enthalpies of water molecules to hydrated clusters containing divalent metal ions with up to 124 water molecules measured under similar conditions indicate that the clusters may have some icelike structure.[30] Thus, the nanodrops in our experiments may be more like amorphous ice than liquid water.

IRPD Spectral Fitting. To more directly compare the IRPD spectra, each spectrum was fit by three optimized Gaussian line shapes with two peaks in the bonded-OH spectral region (2900−3600 cm^{-1}) and one smaller peak near 3700 cm^{-1}. Using only one Gaussian line shape in the H-bonding region results in a significantly worse fit, and three line shapes provide only slightly improved fitting over two. H-bonded features in absorption,[26] Raman,[26] and SFG[63,64] spectra have also been fit with two dominant line shapes and have often been interpreted as corresponding to "icelike" and "liquid-like" water molecules for the lower and higher frequency bands, respectively. However, more recent studies[11,65] indicate that water molecules adopt a continuum of H-bonding environments and that a two-state (or multistate) interpretation of these spectra is misleading. Spectral fitting is used here solely for the purpose of more directly comparing the IRPD spectra of different ions. The experimental data and fits to these data for Ca^{2+} and SO_4^{2-} are shown in Figure 4. From the optimized Gaussian line shapes, peak centroids, intensities, and widths are obtained, and these parameters for the spectrum of each ion are given in Table 1. The free-OH band frequency is red-shifted systematically over a 7 cm^{-1} range and increases in intensity by a factor of 3 with increasing positive charge state of the ion in the nanodrop. The frequencies of the two line shapes fit to the bonded-OH feature each vary by less than 75 cm^{-1} with ion identity. Recent computational models[11,66] for infrared and Raman spectroscopy of aqueous solutions indicate that the

dx.doi.org/10.1021/ja303191r | J. Am. Chem. Soc. 2012, 134, 10228−10236

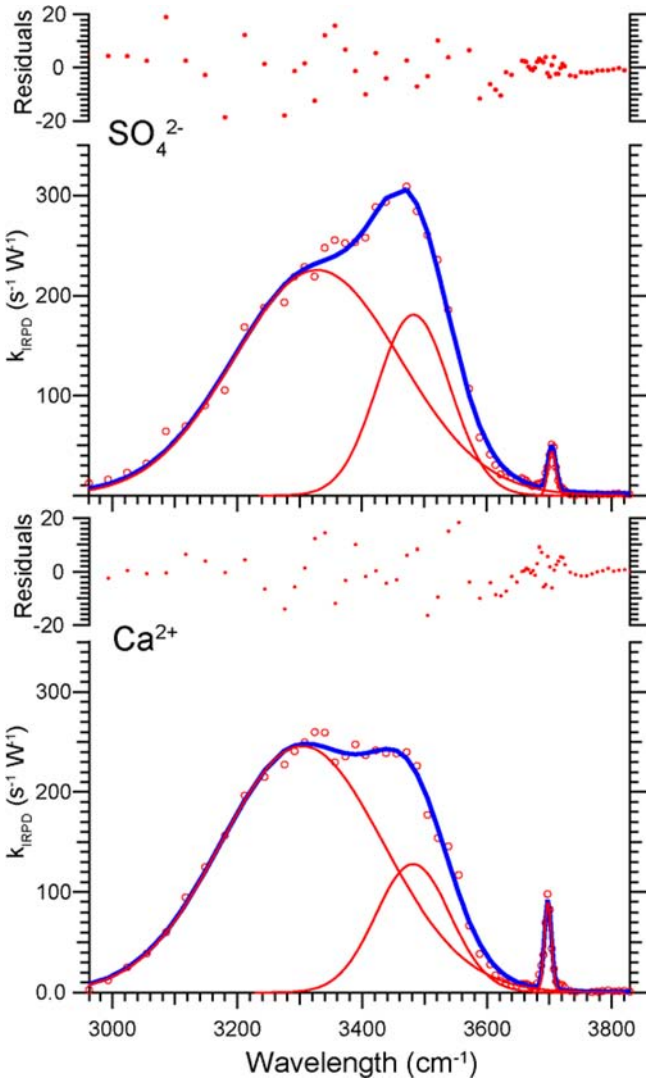

Figure 4. Ensemble IRPD spectra of $M(H_2O)_{\sim 250}$, M = Ca^{2+} and SO_4^{2-} with fitted Gaussian line shapes and the residual values between the total fit and the experimental data.

spectral region from 3500 to 3600 cm^{-1} is associated with water molecules that are less strongly H-bonded than those at lower frequencies. There is a slight red-shift in the centroid of the H-bonded feature with increasing charge state for the cation spectra, and this shift is consistent with the greater polarization of interior water molecules for the more highly charged ions.

Integrated Band Intensities. The IRPD intensity at a given wavelength depends on many factors, including the laser power, the absorption cross section at that frequency, the number of labile surface water molecules, and the dissociation barrier for the loss of a water molecule from the cluster. The internal energy of these clusters is sufficiently high at 133 K that the absorption of even a single photon will result in an increased dissociation rate, although absorption of many photons occurs over the irradiation times used in these experiments. Under these conditions, the IRPD spectra should resemble linear absorption spectra so that the intensities of the bands are roughly proportional to both the oscillator strength and the number of oscillators.

The integrated intensities of these spectra obtained from the fits to the IRPD data as a function of charge state are given in Figure 5. The total integrated intensities of clusters with Na^+ and I^- are similar, indicating that the absorption cross sections and the dissociation barriers for these clusters are similar. The integrated intensities for Ca^{2+}, La^{3+}, and SO_4^{2-} containing nanodrops are higher than those for the monovalent ions. The binding energy of a water molecule in $M^{z\pm}(H_2O)_{250}$, calculated using a continuous Thomson liquid-drop model,[67] is 9.52, 9.58, and 9.67 kcal/mol for singly, doubly, and triply charged ions,

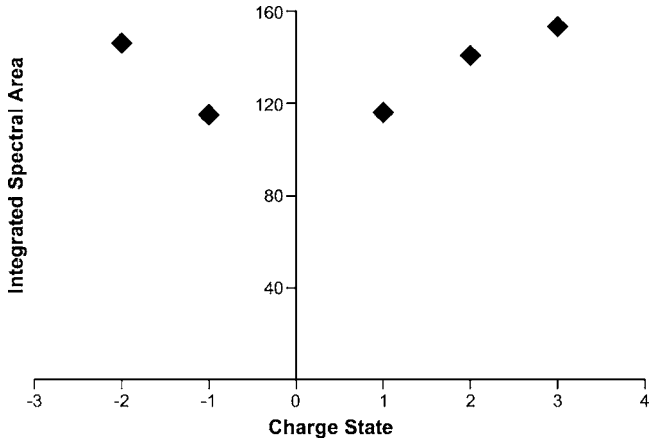

Figure 5. Integrated spectral areas from the ensemble IRPD spectra of $M(H_2O)_{\sim 250}$, M = La^{3+}, Ca^{2+}, Na^+, I^-, and SO_4^{2-} versus ion charge state.

Table 1. Parameters of Gaussian Line Shapes Fit to IRPD Spectra for $M(H_2O)_{\sim 250}$[a]

	SO_4^{2-}	I^-	Na^+	Ca^{2+}	La^{3+}
Band 1					
frequency (cm^{-1})	3330 ± 6	3281 ± 11	3256 ± 14	3305 ± 7	3314 ± 5
intensity (s^{-1} W^{-1})	0.227 ± 0.005	0.171 ± 0.005	0.162 ± 0.006	0.246 ± 0.004	0.258 ± 0.004
width (cm^{-1})	191 ± 7	163 ± 11	165 ± 14	185 ± 8	197 ± 7
Band 2					
frequency (cm^{-1})	3482.4 ± 1.7	3464 ± 4	3459 ± 7	3481 ± 3	3487 ± 2
intensity (s^{-1} W^{1-})	0.18 ± 0.01	0.18 ± 0.02	0.17 ± 0.02	0.12 ± 0.01	0.13 ± 0.01
width (cm^{-1})	81 ± 4	98 ± 5	112 ± 6	83 ± 6	72 ± 6
Band 3					
frequency (cm^{-1})	3704.5 ± 0.8	3702.5 ± 0.7	3698.6 ± 0.7	3697.8 ± 0.4	3697.1 ± 0.3
intensity (s^{-1} W^{-1})	0.044 ± 0.005	0.046 ± 0.005	0.060 ± 0.006	0.089 ± 0.005	0.126 ± 0.007
width (cm^{-1})	9 ± 1	9 ± 1	9 ± 1	8.1 ± 0.5	7.7 ± 0.5

[a]Error values are calculated from the scatter of the experimental data about the fitted line shapes.

dx.doi.org/10.1021/ja303191r | J. Am. Chem. Soc. 2012, 134, 10228−10236

respectively. Although the dissociation barrier increases slightly with charge state, the clusters containing multivalent ions dissociate more readily. The similar dissociation observed for the monovalent ions indicates that the polarity of the ion does not, in the absence of any significant structural effects, have a strong effect on the absorption cross sections of water in these clusters.

Ion Effects on Free-OH Stretch Frequency and Intensity. The frequency of the free-OH band in each spectrum varies nearly linearly with the charge state of the ion in the nanodrop, decreasing from 3704.5 cm^{-1} for $SO_4^{2-}(H_2O)_{\sim 250}$ to 3697.1 cm^{-1} for $La^{3+}(H_2O)_{\sim 250}$ (Figure 6A). A line fit to all these data results in a slope of ~1.5 cm^{-1} per unit charge. A similar linear dependence of the frequency of the free-OH band with charge state was reported previously for ions with ~36 water molecules attached, but the slope for these smaller clusters is ~10× greater.[16] The near linear dependence of frequency with ion charge state is consistent with a Stark effect owing to the electric field at the nanodrop surface that is caused by the ion. The much smaller dependence for clusters with 250 compared to those with 36 water molecules is consistent with a lower electric field strength at the surface of the larger nanodrops due to improved ion solvation and greater average distances between the surface water molecules with free-OH groups and the ion in the nanodrop.

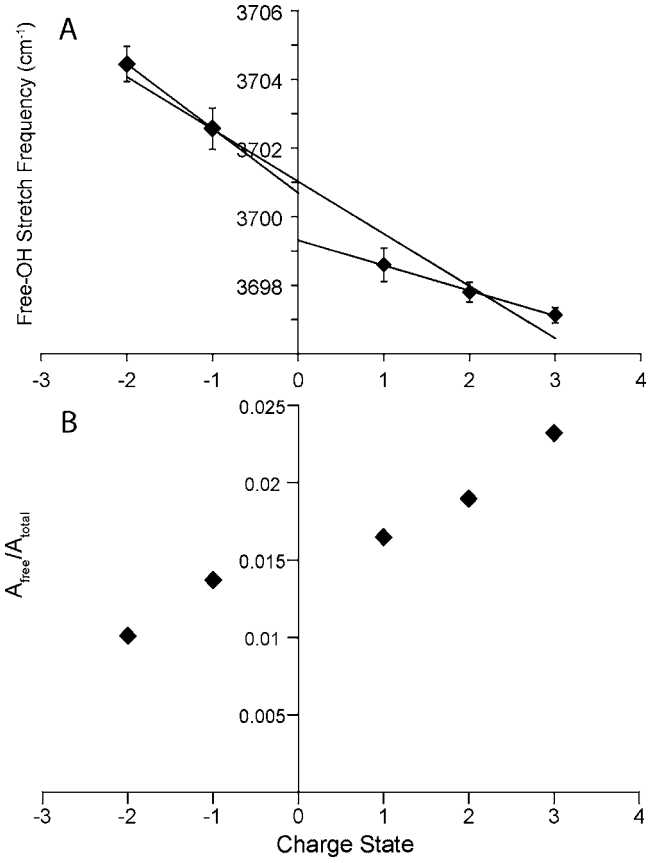

Figure 6. (A) Free-OH stretch frequencies from the ensemble IRPD spectra of $M(H_2O)_{\sim 250}$, M = La^{3+}, Ca^{2+}, Na^+, I^-, and SO_4^{2-}, versus ion charge state. The *R*-squared values for the fits of the cation and total data sets are 0.9974 and 0.9651, respectively. (B) Ratios of the free-OH integrated area (A_{free}) to total integrated area (A_{total}) from the ensemble IRPD spectra of $M(H_2O)_{\sim 250}$, M = La^{3+}, Ca^{2+}, Na^+, I^-, and SO_4^{2-}, versus ion charge state.

As was the case for the clusters with 36 water molecules,[16] data for just the cations are significantly more linear than data that includes both anions and cations. This indicates that the orientation of water molecules at the surface of the clusters that contain cations is similar for each charge state but differs slightly from those at the surface of clusters that contain anions. This suggests that the polarity of the ion in the droplet results in differences in water structure that propagate out to water molecules that are at the surface of these clusters. The relative integrated area of the free-OH band to the H-bonded band determined from the fitted line shapes for each of the ions also depends on charge state (Figure 6B). The relative intensity of this band increases as a function of increasing positive charge of the ion in the nanodrop. This increasing intensity for bands with nearly the same frequency suggests that there are greater populations of AAD water molecules for the more positively charged nanodrops, indicating that ion induced patterning of the hydration structure of these clusters extends to the surface. Although band intensities in small hydrated ion clusters can be affected by the presence of a charge,[47−50] both molecular mechanics simulations as well as a comparison of the Na^+ and I^- data (vide infra) support the conclusion that there are more free-OH groups at the droplet surface with increasingly positive charge.

Although neutral nanodrops cannot be probed in these experiments, an estimate of the free-OH stretch of surface water molecules in a neutral aqueous nanodrop can be obtained by extrapolating the data for charged nanodrops to zero charge. Extrapolation of the cation and anion data to zero charge results in values of 3699.3 and 3700.1 cm^{-1}, respectively, which should be lower and upper bounds for the free-OH band frequency of a similarly sized neutral water cluster. These values are slightly lower than our previously estimated range for the neutral AAD free-OH band frequency (3704.9−3709.7 cm^{-1}) obtained from the IRPD spectra of clusters with 36 water molecules.[16] The discrepancy between the extrapolation at small and large cluster sizes indicates that the structure of water at the surface of the smaller ion-containing clusters differs slightly from that of the larger clusters although effects of the different surface curvatures may also play a role. The value of the free-OH stretch frequency of water on a neutral droplet obtained from the data for the larger clusters is nearly the same as the AAD free-OH band frequencies measured for protonated water clusters (3699.1 cm^{-1}, for $H^+(H_2O)_{200}$)[31] and for large neutral water clusters generated in supersonic expansions, 3693 and 3710 cm^{-1} for the cluster sizes ~16.5 nm and ~1 nm, respectively.[68] It is also consistent with the estimates of bulk water AAD free-OH band frequencies obtained from SFG experiments at room temperature (3690−3705 cm^{-1}),[26,63,69,70] which also show evidence of two types of surface water molecules, although the origin of the band assigned to AD water molecules is debated. The free-OH band measured in SFG experiments is very broad (~50 cm^{-1}), and the SFG band frequency and line shape depend on the polarization and angle of incidence of the incoming laser beams, resulting in a concomitant uncertainty in determining the true free-OH stretch band frequency of a surface water molecule precisely from these measurements. The differing fits for cations and anions suggest that there is a slight effect of the ion polarity on the water molecule orientation at the surface of these very large hydrated clusters, but this effect is relatively small and does not

dx.doi.org/10.1021/ja303191r | J. Am. Chem. Soc. 2012, 134, 10228−10236

likely significantly affect our estimate of the free-OH stretch frequency of surface water molecules in an uncharged nanodrop of this size.

Spectra of Hydrated Monovalent Ions. The IRPD spectra of $Na^+(H_2O)_{\sim 250}$ and $I^-(H_2O)_{\sim 250}$ are similar, with only very subtle differences in the free-OH and H-bonded bands (Figure 7). The intensity of the free-OH band is slightly greater

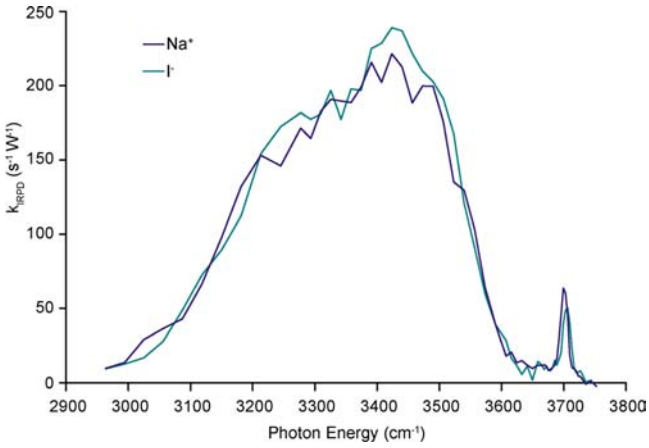

Figure 7. Overlay of the ensemble IRPD spectra of $M(H_2O)_{\sim 250}$, M = Na^+ and I^- at 133 K.

for Na^+ than for I^- whereas the H-bonded band is marginally greater for I^-. Because the integrated intensities of these spectra are essentially the same, this difference in the free-OH band intensity suggests that there are slight differences in the structure of surface water molecules for nanodrops containing Na^+ compared to those containing I^-. In contrast, the free-OH band intensity for Na^+ is approximately double that for I^- for clusters with 36 water molecules,[16] indicating that the structure of water at the surface of the smaller nanodrops depends more strongly on the ion polarity. The similarity of the spectra with ~250 water molecules is consistent with the polarity of the ion having a negligible effect on the transition intensities or the H-bonding network for the majority of water molecules in these larger nanodrops.

Ions of opposite polarity tend to orient water molecules that coordinate directly to the ions differently. Weakly interacting ions, such as tetramethylammonium, have only a small effect on the orientation of solvating water molecules.[32] For most cations, adjacent water molecules align so that the OH groups point away from the ion whereas, for anions, the H atoms generally interact with the anion or oxygen atoms of other water molecules so that the OH groups point inward or are at least tangent to the ion. This difference in hydration orientation can cause substantial differences in the IRPD spectra of many small hydrated cation and anion clusters, especially in the free-OH spectral region. A free OH-band occurs for cations at all cluster sizes. In contrast, there is no free-OH band for many smaller hydrated anion clusters, including I^-, Cl^-, and Br^- with three water molecules.[40] For sulfate dianion, no free-OH band is observed with up to 43 water molecules, indicating that this ion can affect the structure of water well past the first and second solvent shells.[15] Although differences in the H-bonding structure of water may persist past the first and even second solvent shells for nanodrops containing Na^+ and I^- as well, any differences for the majority of water molecules in clusters with 250 water molecules are small.

Spectra of Hydrated Divalent Ions. In contrast to the results for the monovalent ions, there are significant spectral differences between the IRPD spectra of $Ca^{2+}(H_2O)_{\sim 250}$ and $SO_4^{2-}(H_2O)_{\sim 250}$ (Figure 4). For Ca^{2+}, the free-OH band intensity is ~2× greater than that for SO_4^{2-}. This band intensity for the singly charged ions is nearly equal, which indicates that the polarity of the ion has little effect on the transition dipole moments of surface water molecules for clusters of this size. Thus, the greater intensity of this band for Ca^{2+} indicates that there are significantly more free-OH groups at the surface compared to the case for droplets containing SO_4^{2-}. Structures obtained from the molecular dynamics simulations are consistent with these results. On the basis of 1000 calculated structures for each hydrated ion, ~5% of OH groups in nanodrops with SO_4^{2-} are free-OH groups whereas this number is ~10% for Ca^{2+}, consistent with the ~2× more intense free-OH band in the IRPD spectrum of $Ca^{2+}(H_2O)_{\sim 250}$ compared to that for $SO_4^{2-}(H_2O)_{\sim 250}$.

There are also significant differences in the H-bonded region of the spectra for these two ions. For SO_4^{2-}, the dissociation intensity at ~3480 cm^{-1} is ~50% greater than the intensity at ~3300 cm^{-1} whereas the intensities for Ca^{2+} at these energies are within 5% of each other. To confirm the differences in band intensities obtained from the spectral fits, accurate photodissociation rate constants for these two ions were measured at 3340 cm^{-1} and 3475 cm^{-1} (Figure 8). Dissociation rate constants (k_{3340}, k_{3475}, k_{BIRD}) are obtained from linear fits to the dissociation data measured for irradiation times up to 1.25 s

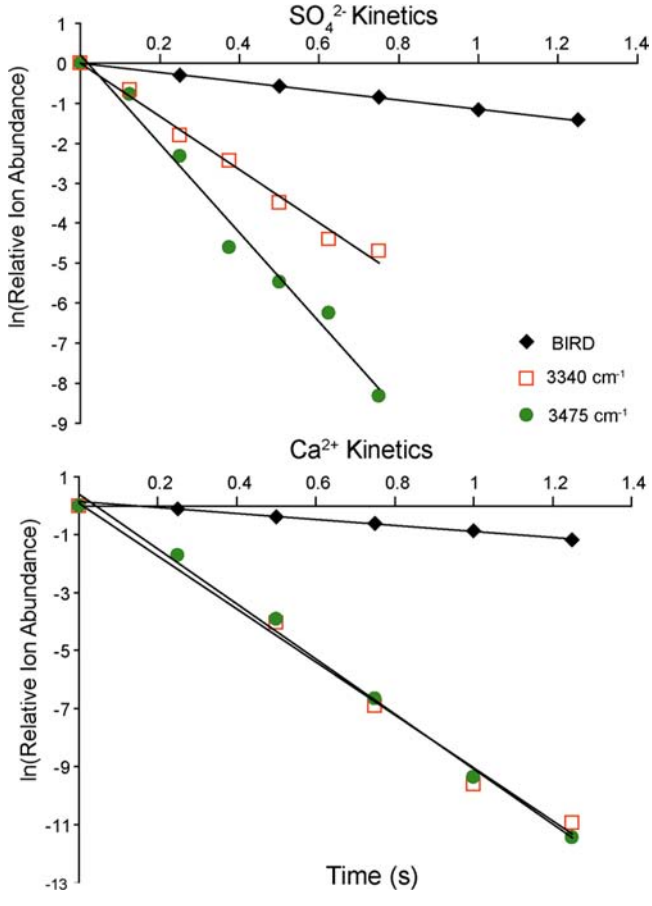

Figure 8. BIRD and laser photodissociation data at ~3340 and 3475 cm^{-1} for $SO_4^{2-}(H_2O)_{\sim 250}$ and $Ca^{2+}(H_2O)_{\sim 250}$ at 133 K.

dx.doi.org/10.1021/ja303191r | J. Am. Chem. Soc. 2012, 134, 10228−10236

(Table 2). Laser-induced dissociation rate constants are determined by subtracting the BIRD rate constant, k_{BIRD}, from the photodissociation rate constants, k_{3340} and k_{3475}. Consistent with the analysis based on the Gaussian fits to the IRPD spectra, the laser-induced dissociation rate constant at 3475 cm^{-1} for SO_4^{2-} is ~2× greater than that at 3340 cm^{-1}. For Ca^{2+}, the laser-induced dissociation rate constant at 3475 cm^{-1} is within 5% of the value at 3340 cm^{-1}.

Table 2. Dissociation Rate Constants (s^{-1}) for $Ca^{2+}(H_2O)_{\sim 250}$ and $SO_4^{2-}(H_2O)_{\sim 250}$

$M(H_2O)_{\sim 250}$	k_{3475} (s^{-1})	k_{3340} (s^{-1})	k_{BIRD} (s^{-1})
Ca^{2+}	9.4 ± 0.3	9.1 ± 0.5	1.04 ± 0.03
SO_4^{2-}	11.1 ± 0.7	6.3 ± 0.3	1.13 ± 0.01

The differences observed in the H-bonded region indicate that the structure of water in the interior of the droplets differs when the nanodrop contains SO_4^{2-} vs Ca^{2+}. For cations, the red-shift in the centroid of the fully H-bonded feature indicates greater polarization of the interior water molecules with increasing charge state. However, the spectra for I^- and SO_4^{2-} indicate the opposite trend and the faster dissociation at ~3480 cm^{-1} for SO_4^{2-} indicates an increased population of more weakly H-bonded water molecules relative to those in the Ca^{2+} hydrated clusters. This difference is likely due to the competition between ion-induced water patterning and intrinsic water−water interactions. For cations, both the ion-induced patterning and intrinsic water−water interactions orient water molecules such that OH groups tend to point away from the ion. However, as indicated by the increasing free-OH band intensity with increasing cluster size in IRPD spectra of SO_4^{2-} clusters with ~43−80 water molecules,[15] anion-induced patterning of water molecules competes with the intrinsic water−water interactions, orienting molecules close to the ion such that the OH groups point inward. This competition may result in a strain on the H-bond network and a larger population of more weakly H-bonded water molecules for anions with extensive ion-induced water patterning.

Hydrated Trivalent Ions. Although nanodrops containing positively charged trivalent ions that exist in bulk solution can be readily formed and probed with IRPD spectroscopy, nanodrops containing small trivalent anions have not yet been observed. Thus, we are unable to directly compare the IRPD spectra of trivalent ions of opposite polarity. However, we can draw some conclusions about the effects of ion valency from the comparison of the IRPD spectra of $La^{3+}(H_2O)_{\sim 250}$ with those of the other ions. The free-OH band for La^{3+} is the most intense of any of the ions (Figure 3), consistent with this cluster having the largest number of water molecules with a free-OH stretch. The total integrated area (A_{total}) over both the bonded and free O−H stretch regions for La^{3+} is greater than that for the monovalent ions and for Ca^{2+}, but it is close to that for SO_4^{2-} (Figure 5). For hydrated La^{3+} clusters, the water molecules are more tightly bound than for Na^+ at equivalent cluster size. However, A_{total} for La^{3+} is greater than that for Na^+, the opposite of the order expected on the basis of the slightly lower water binding energy for Na^+. This indicates that the difference in A_{total} may be the result of differences in the H-bonding network of water molecules in these clusters. At some cluster size, the interactions between the majority of water molecules should not depend on the identity of the ion in the cluster. The similarity of the IRPD spectra of $M(H_2O)_{\sim 250}$, M = Na^+ and I^-, indicates that the majority of water molecules are not significantly affected by these ions whereas the spectra for M = La^{3+}, Ca^{2+}, and SO_4^{2-} indicate that much larger water clusters are required for this to be the case for multivalent ions.

CONCLUSIONS

The IRPD spectra of aqueous nanodrops consisting of ~250 water molecules and either SO_4^{2-}, I^-, Na^+, Ca^{2+}, or La^{3+} were measured to determine the effect of the ion on the H-bonded structure of water both in the interior of the droplet and at the droplet surface. Free-OH stretches corresponding to water molecules at the nanodrop surface that accept two H-bonds and donate a single H-bond red-shift with increasingly positive charge, consistent with a Stark effect as a result of the ion's electric field at the droplet surface. A small difference between this Stark shift for droplets containing anions compared to those that contain cations is consistent with a subtle difference in the orientation of water molecules at the surface of the nanodrops containing ions of opposite polarity. A clear trend in increasing intensity of this peak with increasing positive charge on the nanodrop is consistent with more water molecules with free-OH stretches at the surfaces of the more positively charged nanodrops.

The spectra of nanodrops with Na^+ and I^- are very similar, which indicates that the H-bonding network of the majority of water molecules is very similar for these monovalent ions despite differences that likely exist in the first and possibly second solvation shells. In contrast, the IRPD spectra of nanodrops containing SO_4^{2-} and Ca^{2+} are significantly different both in the free-OH stretch region and in the H-bonding region. These results indicate that these divalent ions can affect the H-bonding network of water molecules not only in the interior but also at the surface of the droplet itself. The number of water molecules in the first solvation shell of either ion is relatively small compared to the overall number of water molecules. In addition, the differences in the H-bonding region occur in the higher frequency region of the spectrum where inner shell water molecules should not contribute significantly. Thus, these results provide compelling evidence that these ions affect the structure of fully H-bonded water molecules well past the first solvation shell.

In contrast to conclusions from many other studies, these results indicate that ions can have a significant and readily measured effect on the structure of water, even for water molecules that are remote from the ion. Although our earlier studies showed that SO_4^{2-} can significantly affect the structure of water at the surface of droplets with as many as 43 water molecules,[15] which is well past the second solvation shell, this effect is expected to be mitigated in dilute bulk solution because of H-bonding to other water molecules that are even more remote from the ion. The results here for clusters with ~250 water molecules show that the H-bonding network of water molecules in the second or even third solvation shell that are fully H-bonded, *as they would be in bulk solution*, is also affected. These results provide new insights into ion hydration and how ions may affect various physical properties, including Hofmeister effects.

These are the largest mass selected ionic clusters for which IRPD spectra have been reported to date. Additional studies on even larger ion-containing nanodrops made possible by the higher magnetic field strength of the FT/ICR apparatus should provide even more detailed information about ion−water interactions. For example, what is the size of a nanodrop where

dx.doi.org/10.1021/ja303191r | J. Am. Chem. Soc. 2012, 134, 10228−10236

ions no longer measurably affect the H-bonding structure of surface water molecules? How does the presence of a counterion in the nanodrop affect the H-bonding network of water? We anticipate the answers to these and many other interesting questions will be forthcoming.

AUTHOR INFORMATION

Corresponding Author

williams@cchem.berkeley.edu

Notes

The authors declare no competing financial interest.

ACKNOWLEDGMENTS

The authors wish to thank Dr. James S. Prell for many helpful discussions and useful suggestions, the National Science Foundation (Grant CHE-1012833) for generous financial support, and the Boehringer Ingelheim Cares Foundation for donation of the 7.0 T superconducting magnet used in this research.

REFERENCES

(1) Hofmeister, F. *Arch. Exp. Pathol. Pharmacol.* **1888**, *25*, 1−30.
(2) Hofmeister, F. *Arch. Exp. Pathol. Pharmacol.* **1887**, *24*, 247−260.
(3) Kunz, W.; Henle, J.; Ninham, B. W. *Curr. Opin. Colloid Interface Sci.* **2004**, *9*, 19−37.
(4) Collins, K. D. *Biophys. J.* **1997**, *72*, 65−76.
(5) Schott, H. J. *Colloid Interface Sci.* **1973**, *43*, 150−155.
(6) Grigorjev, P. A.; Bezrukov, S. M. *Biophys. J.* **1994**, *67*, 2265−2271.
(7) Uejio, J. S.; Schwartz, C. P.; Duffin, A. M.; Drisdell, W. S.; Cohen, R. C.; Saykally, R. J. *Proc. Natl. Acad. Sci. U. S. A.* **2008**, *105*, 6809−6812.
(8) Freire, M. G.; Neves, C. M. S. S.; Silva, A. M. S.; Santos, L. M. N. B. F.; Marrucho, I. M.; Rebelo, L. P. N.; Shah, J. K.; Maginn, E. J.; Coutinho, J. A. P. *J. Phys. Chem. B* **2010**, *114*, 2004−2014.
(9) Chen, X.; Yang, T.; Kataoka, S.; Cremer, P. S. *J. Am. Chem. Soc.* **2007**, *129*, 12272−12279.
(10) Algaer, E. A.; van der Vegt, N. F. A. *J. Phys. Chem. B* **2011**, *115*, 13781−13787.
(11) Smith, J. D.; Saykally, R. J.; Geissler, P. L. *J. Am. Chem. Soc.* **2007**, *129*, 13847−13856.
(12) Lin, Y. S.; Auer, B. M.; Skinner, J. L. *J. Chem. Phys.* **2009**, *131*, 144511.
(13) Collins, K. D. *Methods* **2004**, *34*, 300−311.
(14) Pegram, L. M.; Record, M. T. *J. Phys. Chem. B* **2007**, *111*, 5411−5417.
(15) O'Brien, J. T.; Prell, J. S.; Bush, M. F.; Williams, E. R. *J. Am. Chem. Soc.* **2010**, *132*, 8248−8249.
(16) Prell, J. S.; O'Brien, J. T.; Williams, E. R. *J. Am. Chem. Soc.* **2011**, *133*, 4810−4818.
(17) Flick, T. G.; Merenbloom, S. I.; Williams, E. R. *J. Am. Soc. Mass Spectrom.* **2011**, *22*, 1968−1977.
(18) Baldwin, R. L. *Biophys. J.* **1996**, *71*, 2056−2063.
(19) Cacace, M. G.; Landau, E. M.; Ramsden, J. J. *Q. Rev. Biophys.* **1997**, *30*, 241−277.
(20) Cheng, J.; Vecitis, C. D.; Hoffmann, M. R.; Colussi, A. J. *J. Phys. Chem. B* **2006**, *110*, 25598−25602.
(21) Omta, A. W.; Kropman, M. F.; Woutersen, S.; Bakker, H. J. *J. Chem. Phys.* **2003**, *119*, 12457−12461.
(22) Omta, A. W.; Kropman, M. F.; Woutersen, S.; Bakker, H. J. *Science* **2003**, *301*, 347−349.
(23) Tielrooij, K. J.; Garcia-Araez, N.; Bonn, M.; Bakker, H. J. *Science* **2010**, *328*, 1006−1009.
(24) Tielrooij, K. J.; van der Post, S. T.; Hunger, J.; Bonn, M.; Bakker, H. J. *J. Phys. Chem. B* **2011**, *115*, 12638−12647.
(25) Liu, D. F.; Ma, G.; Levering, L. M.; Allen, H. C. *J. Phys. Chem. B* **2004**, *108*, 2252−2260.
(26) Gopalakrishnan, S.; Jungwirth, P.; Tobias, D. J.; Allen, H. C. *J. Phys. Chem. B* **2005**, *109*, 8861−8872.
(27) Jungwirth, P. *Faraday Discuss.* **2009**, *141*, 9−30.
(28) Donald, W. A.; Leib, R. D.; Demireva, M.; O'Brien, J. T.; Prell, J. S.; Williams, E. R. *J. Am. Chem. Soc.* **2009**, *131*, 13328−13337.
(29) Griffin, G. B.; Young, R. M.; Ehrler, O. T.; Neumark, D. M. *J. Chem. Phys.* **2009**, *131*, 194302.
(30) Donald, W. A.; Leib, R. D.; Demireva, M.; Negru, B.; Neumark, D. M.; Williams, E. R. *J. Phys. Chem. A* **2011**, *115*, 2−12.
(31) Mizuse, K.; Mikami, N.; Fujii, A. *Angew. Chem., Int. Ed.* **2010**, *49*, 10119−10122.
(32) Prell, J. S.; Williams, E. R. *J. Am. Chem. Soc.* **2009**, *131*, 4110−4119.
(33) Chang, H. C.; Wang, Y. S.; Lee, Y. T. *Int. J. Mass Spectrom.* **1998**, *180*, 91−102.
(34) Choi, J. H.; Kuwata, K. T.; Cao, Y. B.; Okumura, M. *J. Phys. Chem. A* **1998**, *102*, 503−507.
(35) Headrick, J. M.; Diken, E. G.; Walters, R. S.; Hammer, N. I.; Christie, R. A.; Cui, J.; Myshakin, E. M.; Duncan, M. A.; Johnson, M. A.; Jordan, K. D. *Science* **2005**, *308*, 1765−1769.
(36) Iino, T.; Ohashi, K.; Inoue, K.; Judai, K.; Nishi, N.; Sekiya, H. *J. Chem. Phys.* **2007**, *126*, 194302.
(37) Miller, D. J.; Lisy, J. M. J. *Am. Chem. Soc* **2008**, *130*, 15381−15392.
(38) Miyazaki, M.; Fujii, A.; Ebata, T.; Mikami, N. *Science* **2004**, *304*, 1134−1137.
(39) Nicely, A. L.; Miller, D. J.; Lisy, J. M. *J. Mol. Spectrosc.* **2009**, *257*, 157−163.
(40) Robertson, W. H.; Johnson, M. A. *Annu. Rev. Phys. Chem.* **2003**, *54*, 173−213.
(41) Shin, J. W.; Hammer, N. I.; Diken, E. G.; Johnson, M. A.; Walters, R. S.; Jaeger, T. D.; Duncan, M. A.; Christie, R. A.; Jordan, K. D. *Science* **2004**, *304*, 1137−1140.
(42) Walters, R. S.; Pillai, E. D.; Duncan, M. A. *J. Am. Chem. Soc.* **2005**, *127*, 16599−16610.
(43) Ayotte, P.; Bailey, C. G.; Weddle, G. H.; Johnson, M. A. *J. Phys. Chem. A* **1998**, *102*, 3067−3071.
(44) Ayotte, P.; Weddle, G. H.; Bailey, C. G.; Johnson, M. A.; Vila, F.; Jordan, K. D. *J. Chem. Phys.* **1999**, *110*, 6268−6277.
(45) Beck, J. P.; Lisy, J. M. *J. Chem. Phys.* **2011**, *135*, 044302.
(46) Cabarcos, O. M.; Weinheimer, C. J.; Lisy, J. M.; Xantheas, S. S. *J. Chem. Phys.* **1999**, *110*, 5−8.
(47) Bandyopadhyay, B.; Duncan, M. A. *Chem. Phys. Lett.* **2012**, *530*, 10−15.
(48) Carnegie, P. D.; Bandyopadhyay, B.; Duncan, M. A. *J. Phys. Chem. A* **2008**, *112*, 6237−6243.
(49) Carnegie, P. D.; Bandyopadhyay, B.; Duncan, M. A. *J. Chem. Phys.* **2011**, *134*, 014302.
(50) Carnegie, P. D.; Bandyopadhyay, B.; Duncan, M. A. *J. Phys. Chem. A* **2011**, *115*, 7602−7609.
(51) Bush, M. F.; O'Brien, J. T.; Prell, J. S.; Wu, C. C.; Saykally, R. J.; Williams, E. R. *J. Am. Chem. Soc.* **2009**, *131*, 13270−13277.
(52) Bush, M. F.; Saykally, R. J.; Williams, E. R. *ChemPhysChem* **2007**, *8*, 2245−2253.
(53) Bush, M. F.; Saykally, R. J.; Williams, E. R. *J. Am. Chem. Soc.* **2007**, *129*, 2220−2221.
(54) Bush, M. F.; Saykally, R. J.; Williams, E. R. *J. Am. Chem. Soc.* **2008**, *130*, 15482−15489.
(55) Cooper, T. E.; O'Brien, J. T.; Williams, E. R.; Armentrout, P. B. *J. Phys. Chem. A* **2010**, *114*, 12646−12655.
(56) O'Brien, J. T.; Williams, E. R. *J. Phys. Chem. A* **2008**, *112*, 5893−5901.
(57) O'Brien, J. T.; Williams, E. R. *J. Phys. Chem. A* **2011**, *115*, 14612−14619.
(58) Bush, M. F.; Saykally, R. J.; Williams, E. R. *J. Am. Chem. Soc.* **2008**, *130*, 9122−9128.
(59) Bush, M. F.; O'Brien, J. T.; Prell, J. S.; Saykally, R. J.; Williams, E. R. *J. Am. Chem. Soc.* **2007**, *129*, 1612−1622.

(60) Prell, J. S.; O'Brien, J. T.; Williams, E. R. *J. Am. Soc. Mass Spectrom.* **2010**, *21*, 800−809.
(61) Schriver-Mazzuoli, L.; Schriver, A.; Hallou, A. *J. Mol. Struct.* **2000**, *554*, 289−300.
(62) Manka, A.; Pathak, H.; Tanimura, S.; Wolk, J.; Strey, R.; Wyslouzil, B. E. *Phys. Chem. Chem. Phys.* **2012**, *14*, 4505−4516.
(63) Du, Q.; Superfine, R.; Freysz, E.; Shen, Y. R. *Phys. Rev. Lett.* **1993**, *70*, 2313−2316.
(64) Du, Q.; Freysz, E.; Shen, Y. R. *Science* **1994**, *264*, 826−828.
(65) Tian, C. S.; Shen, Y. R. *Chem. Phys. Lett.* **2009**, *470*, 1−6.
(66) Yang, M.; Skinner, J. L. *Phys. Chem. Chem. Phys.* **2010**, *12*, 982−991.
(67) Donald, W. A.; Williams, E. R. *J. Phys. Chem. A* **2008**, *112*, 3515−3522.
(68) Buch, V.; Bauerecker, S.; Devlin, J. P.; Buck, U.; Kazimirski, J. K. *Int. Rev. Phys. Chem.* **2004**, *23*, 375−433.
(69) Ji, N.; Ostroverkhov, V.; Tian, C. S.; Shen, Y. R. *Phys. Rev. Lett.* **2008**, *100*, 096102.
(70) Raymond, E. A.; Richmond, G. L. *J. Phys. Chem. B* **2004**, *108*, 5051−5059.